

Systematic evolution of charge radii along $Z = 98-120$ isotopic chains

Rong An,^{1,2,*} Xiao-Xu Dong,³ and Feng-Shou Zhang^{4,2,5,†}

¹*Key Laboratory of Beam Technology of Ministry of Education,
Institute of Radiation Technology, Beijing Academy
of Science and Technology, Beijing 100875, China*

²*Key Laboratory of Beam Technology of Ministry of Education,
College of Nuclear Science and Technology,
Beijing Normal University, Beijing 100875, China*

³*School of Physics, Beihang University, Beijing 102206, China*

⁴*Key Laboratory of Beam Technology of Ministry of Education,
Beijing Radiation Center, Beijing 100875, China*

⁵*Center of Theoretical Nuclear Physics,
National Laboratory of Heavy Ion Accelerator of Lanzhou, Lanzhou 730000, China*

Abstract

In this work, the evolution of nuclear charge radii along even $Z = 98 - 120$ isotopes are systematically investigated by various approaches. The new parametrization sets based on liquid drop model (LDM) formulas are proposed by covering the shell closure effect at $N = 126$ and odd-even staggering (OES) in calibration procedure. In comparison with available database, high-order neutron-proton asymmetry may be indispensable in fitting protocol. The fitted formula within theoretical uncertainty below 0.02 fm is used to make extrapolative calculations. Results obtained by the deduced relationship associating to α -decay properties and the modified charge radius formula in relativistic mean field (RMF) model are also employed to make reinforce. The latter shows that the abrupt change of nuclear charge radii emerges apparently across $N = 184$ shell closure. In addition, the abrupt jumps at $N = 146$ and 200 are also disclosed remarkably due to the large deformation. These different methods give comparable predictions of nuclear charge radii for $^{286,288}\text{Fl}$, $^{290,292}\text{Lv}$ and $^{288-310}120$ isotopes.

* E-mail: anrong@brc.ac.cn

† E-mail: fszhang@bnu.edu.cn

I. INTRODUCTION

The systematic global evolution of nuclear charge radii along isotopic chains is a hot topic in recent studies. The knowledge of nuclear size plays an important role not only in understanding new physics beyond standard model (SM) [1] but also serving as input quantities in astrophysical study [2]. Besides, available data of charge density distributions of a nucleus can provide a stringent constraint on the equation of state (EoS) [3, 4].

With the development of high intensity ion beam facilities and the advanced detectors, extensive efforts were devoted to the synthesis of superheavy nuclei (SHN) and then the landscape of nuclear chart has been extended to $Z = 118$ in laboratories [5, 6]. Although plenty of methods were undertaken to extract the nuclear size, such as high-energy elastic electron scattering (e^-) [7, 8], muonic atom X-rays (μ^-) [9–11], highly-sensitive Collinear Resonance Ionization Spectroscopy (CRIS) [12, 13], optical isotopes shift (OIS) and K_α X-rays isotopes shift (K_α IS) [14], the research on charge radii of SHN is sort of beyond the ability of available experimental tools due to the quite short lifetimes.

The average trend of nuclear charge radii is usually described by $A^{1/3}$ or $Z^{1/3}$ law due to the consideration of nuclear saturation property [15]. Fruitful experimental data show that shell closure effects and the sizable local variations of charge radii are observed generally throughout the whole nuclear chart [16, 17]. Remarkably in calcium isotopes, nuclear charge radii feature a distinct aspect of odd-even staggering (OES) [18, 19]. Furthermore, this conspicuous feature of the odd-even oscillations in charge radii is still observed apparently along mercury [20] and lead [21] isotopes, etc. Along isotopic chains, abrupt changes in the nuclear charge radii are usually observed. A rapid increase is presented naturally across neutron magic numbers due to shell effect; this leads to the well-known kinks phenomena at $N = 28, 50, 82$ and 126 [16, 17, 19, 22–25]. The other sharp increase is associated to the deformation phase transitions, such as the onset of deformation at $N = 60$ and $N = 90$ regions [26–28]. These irregular and universal behaviors challenge the theoretical models in nuclear physics.

The mean field theory makes a considerable success in describing the fundamental properties of finite nuclei [29]. The charge density distributions are calculated in a self-consistent way based on mean field approaches, such as the relativistic mean field (RMF) theory [30–34] and non-relativistic Hartree-Fock-Bogoliubov (HFB) model [35, 36]. *Ab initio* many-body

calculations with chiral effective field theory (EFT) interactions were also employed to investigate the nuclear charge radii [37–39]. However, the difficulty was encountered in heavy or superheavy regions due to the limitation of computing power. Recently developed Bayesian neural networks (BNNs) are devoted to accurate predictions of nuclear charge radii [40, 41]. Toward superheavy regions, the extrapolative power is poorly achieved due to the absence of database. Besides, many analytical formulas are proposed to evaluate the general trend of nuclear size.

The synthesis of SHN emerges out of understanding of astrophysical process. The production cross sections in SHN is evidently low in experimental and theoretical studies [42]. The main reason is that the fundamental properties of SHN are not clear, especially for the nuclear size. As mentioned in Ref. [24], nuclear charge radii present global and simple patterns along isotopic chains. The objective of this article is to extract root mean square (rms) charge radii of even $Z = 98-120$ isotopes within various approaches. Analytical formulas with new parametrization sets are proposed by covering the OES and shell closure effect. The deduced relation coming from the α -decay properties [43] and the recently developed RMF(BCS)* approach [44] are also employed to investigate the evolution of nuclear charge radii.

This paper is organized as follows. In Sec. II, we briefly describe the theoretical models including the algebraic expressions deduced from the liquid drop model, deduced relation deriving from the α -decay properties and the relativistic mean field approach. Sec. III is devoted to the results and discussions. A short summary and outlook are provided in Sec. IV.

II. THEORETICAL APPROACHES

In recent years, plenty of information about the charge radii of nuclei far away from the β -stability line has become accessible thanks to the advent and development of the highly sensitive radioactive ion beam facilities [16, 17]. Since these available data provide a rigorous benchmark to test and further advance those models of the nuclear theory. Available descriptions of charge radii of SHN play an important role in recognizing the r-process and serving as useful guide in the synthesis of superheavy elements. Therefore various promising candidates were proposed for describing the global variations of charge radii of superheavy nuclei (SHN).

A. Analytical formulas with mass number

The evolution of root-mean square (rms) charge radius can be described by liquid drop model (LDM) formula that builds the relationship between the nuclear size and the corresponding mass number [16], namely

$$R_{\text{ch}} = (a + bA^{-2/3} + cA^{-4/3}) \times A^{1/3}, \quad (1)$$

where $a = 0.9071$ fm, $b = 1.105$ fm and $c = -0.548$ fm, A is nucleus mass number. The rms deviation falls to 5.514×10^{-2} fm by calculating the database profile. As shown in Refs. [45–47], the nuclear size is fairly determined by introducing isospin freedom, namely neutron-proton asymmetry. The equivalent form was shown in Ref. [48] but the neutron-proton asymmetry was introduced as follows,

$$R_{\text{ch}} = r_0(1 - aI + b/A) \times A^{1/3}, \quad (2)$$

where $r_0 = 1.2347$ fm, $a = 0.1428$ and $b = 2.0743$, $I = (N - Z)/A$ is the reduced isospin. The rms deviation falls to 4.96×10^{-2} fm. The four-parameters formula including the high-order neutron-proton asymmetry was written as [49]:

$$R_{\text{ch}} = a + bA^{1/3} + cI + dA^{1/3}I^2, \quad (3)$$

where $a = 0.4980$, $b = 0.8754$, $c = -0.9845$ and $d = 0.2703$ in units of fm. The fit produces the moderate rms deviation of 4.07×10^{-2} fm. These alternative formulas were widely used to make extrapolation in describing nuclear charge radius.

Although these algebraic expressions provide a simple method for estimating nuclear charge radii, the fine details of nuclear structure cannot be covered well. However, as a prior constraint relation, a available formula is necessary in the simulations of machine learning process [41, 50].

B. Nuclear size derived from α -decay properties

The bulk properties of heavy neutron-rich nuclei are hardly determined in experiment due to their short lifetimes [42]. The scattering method is not available because the half-lives of the target nuclei is very short. The α -decay or cluster and proton emissions provide an alternative method for investigating nuclear size [43, 51]. The formula of nuclear rms

charge radii associates to the α -decay properties, such as α -decay energy and the logarithm of α -decay half-lives, is then established as

$$R_{\text{ch}} = \left[(a - b \log_{10} T_{1/2}) / \xi_1 \xi_2 + c \xi_1 / \sqrt{Q_\alpha} \right]^2, \quad (4)$$

where $\xi_1 = \sqrt{Z_c Z_d e^2}$ and $\xi_2 = \sqrt{2\mu}/\hbar$ with reduced mass of the α -daughter system $\mu = A_c A_d / (A_c + A_d)$, $Z_{c,d}$ and $A_{c,d}$ corresponds to the atomic mass number of α and daughter nucleus, respectively. Based on the available charge radii of even-even nuclei with $Z \geq 82$ and $N \geq 126$, the parameters $a = -15.8767$, $b = 0.6213$ and $c = 0.7975$ are determined through the least-square fit process. The standard deviation of the calculation falls to $\sigma = 0.0557$ fm, and more details are shown in Ref. [43]. In this work, charge radii of even-even nuclei are obtained by this deduced relationship.

C. RMF(BCS)* approach

Many nuclear phenomena can be described well by the covariant density functional theory (CDFT) [52–62]. The recently developed ansatz based on the non-linear Lagrangian density was employed to focus on the evolution of nuclei size [44]. The semi-microscopic correction term was introduced into nuclear charge radii formula. The modified mean-square charge radius, labels as RMF(BCS)* approach, is written as follows:

$$R_{\text{ch}}^2 = \frac{\int r^2 \rho_p(\mathbf{r}) d^3r}{\int \rho_p(\mathbf{r}) d^3r} + 0.64 \text{ fm}^2 + \frac{a_0}{\sqrt{A}} |\Delta\mathcal{D}| \text{ fm}^2. \quad (5)$$

Where the first term represents the charge density distributions of point-like proton and then the second term accounts for the finite size of proton [63, 64]. In which the last modified term $a_0 = 0.22$ is an fixed parameter and A represents mass number of a nucleus. $|\Delta\mathcal{D}|$ originates from the differences of measuring Cooper pair components between neutrons and protons.

The modified term whose presence in this expression is firstly mandatory for describing the odd-even oscillations of nuclear charge radii along calcium and potassium isotopic chains [44, 65]. Besides, the abrupt changes of nuclear charge radii across shell closures can also be reproduced well [66]. This introduced term is obtained self-consistently by resolving the state-dependent BCS equations with a δ -force interaction [30]. The pairing strength $V_0 = 322.8 \text{ MeV fm}^3$ is employed for all calculations [44]. NL3 force is especially favorable

to the calculation of charge radii along a long isotopic chain [67]. Actually, parametrization set PK1 and NL3* cannot change the conclusions in quantitative level [66].

The evolution of charge radii is reproduced remarkably well including kinks at magic neutron numbers and OES behaviors. This modified item is explained phenomenologically by the neutron-proton short range correlations (np-SRCs) around Fermi surface. As demonstrated in Ref. [68], np-SRCs can influence the calculated rms nuclear charge radii, but it is invalid for some cases. Especially in our recent works [69], this ansatz has almost no influence in describing some nuclei with open proton shell due to the strong coupling between different levels around Fermi surface, this is in accordance with Miller's [68]. As argued in Ref. [70], this modified formula can improve the description of nuclear charge radii well, but the accepted truth is that this term cannot be included self-consistently in conventional density functional theories (DFTs). Although the underlying physical meaning of this ansatz is not clear, its predictive power is non-negligible.

III. RESULTS AND DISCUSSIONS

A. Odd-even staggering in nuclear charge radii

As well known, the OES behaviors are generally observed in nuclear chart [16, 17]. The source of OES behavior is demonstrated by various possible mechanisms [70], such as the staggering oscillation in occupation of single-particle levels between odd and even isotopes [20] and the pairing contributions [23]. Besides, OES in the charge radii might be related to the evolution of nuclear deformation [71], etc. Although this physical source is complex, introducing OES term is indispensable in analytical expressions.

As shown in Ref. [72, 73], the three-point OES formula is employed to visually measure those local variations of nuclear charge radii. It is written as follows,

$$\Delta_r(N, Z) = [R(N - 1, Z) - 2R(N, Z) + R(N + 1, Z)]/2, \quad (6)$$

where $R(N, Z)$ is the rms charge radius of a nucleus with neutron number N and proton number Z .

In Fig. 1, absolute values of $\Delta_r(N, Z)$ are shown as an function of mass number A . The amplitudes of OES behaviors are gradually weaken with the increasing mass number. However, around $N = 60$ and 90 regions, the enlarged amplitudes are indicated due to the

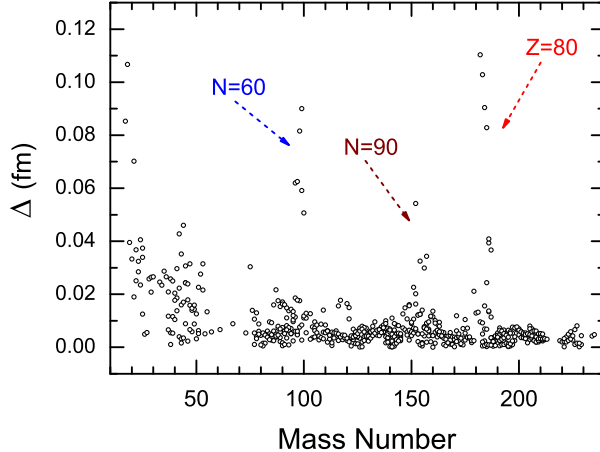


FIG. 1. The absolute values (open circle) of odd-even staggering in nuclear charge radii (defined as $\Delta_r(N, Z)$) are obtained by the three-point formula Eq. (6). The deformation phase transition and shape staggering regions are highlighted by colored arrows.

sudden onset of strong static deformations [26–28]. A strong peak at $N = 90$ can also be clearly seen in the Brix-Kopfermann diagram, which provides a widely applicable prototype for the onset of deformation throughout heavy nuclei [74]. Moreover the large amplitudes of OES can also be encountered in Hg isotopes around neutron-deficient regions due to the shape evolution [75, 76], namely a large and abrupt shape transition from prolate to oblate and again back to prolate. The same scenario can also be encountered in bismuth isotopes [77]. The onset of deformation has been explained as due to the descent of the $h_{9/2}$ “intruder” configuration which destroys the $Z = 82$ gap, and therefore increases the effective number of valence protons [78].

The empirical averaging energy gap on mass number obtained by three-point formula shows the similar trends but with larger magnitudes, and roughly equals to $12/\sqrt{A}$ [79]. In Ref. [44], the modified formula includes similar expression, $\propto 1/\sqrt{A}$, to capture the OES in charge radii. Thus the modified term which includes the form $g \times (-1)^{o,e}/\sqrt{A}$ is introduced into these analytical expressions. Here letter o and e correspond to odd and even neutron numbers, respectively.

In order to investigate the charge radii of even $Z = 98-120$ isotopes and avoid the structure information encountered in light regions, the parameter g is fitted by performing the database with proton number $Z \geq 80$ [16, 17]. Meanwhile, the data of shape staggering are excluded.

In a word, we do want to obtain the charge radius formula with smaller rms deviation and make a powerful extrapolation for superheavy nuclei. The standard deviation between $R_{\text{expt.}}$ and $R_{\text{calc.}}$ is calculated as follows:

$$\sigma = \left[\sum_{i=1}^N (R_{\text{expt.}}^i - R_{\text{calc.}}^i)^2 / N \right]^{1/2}, \quad (7)$$

where the number of data is $N = 192$.

In order to highlight the local variations of nuclear charge radii, the OES and shell effects are introduced in analytical formulas. The new formalism is proposed based on Eq. (1) as follows,

$$R_{\text{ch}} = (a + bA^{-2/3} + cA^{-4/3}) \times A^{1/3} + d(N - N^*)A^{-1/2} + g(-1)^{o.e}A^{-1/2}, \quad (8)$$

where $a = 0.9872$, $b = -1.7067$ and $c = -0.548$, $d = -0.1606$ and $g = 0.0306$ in unit of fm, the standard rms deviation is $\sigma = 3.2 \times 10^{-2}$ fm. Modified term containing form $(N - N^*)A^{-1/2}$ is introduced to highlight the shell effect and N^* represents the reference nuclei with neutron number $N = 126$. A detailed description of the fitting protocol which involving the Casten factor P can also describe the shell effects [80–82]. In which the valence protons and neutrons were contributed to the variations of nuclear size, namely neutron-proton (np) interactions. This means the np interactions play a essential role in describing the fine structure of nuclear charge radii. To summarize, the introduced scheme offers the promise of a much simplified and reliable technique to estimate the charge radii of nuclei stay and far off the β -stability line.

For Eq. (2), the modified form is expressed below:

$$R_{\text{ch}} = r_0(a + bI + c/A) \times A^{1/3} + d(N - N^*)A^{-1/2} + g(-1)^{o.e}A^{-1/2}, \quad (9)$$

where $r_0 = 0.9862$ fm, $a = 1.0607$ and $b = -0.2691$, $c = -8.3617$, $d = 0.0171$ fm, $g = 0.0092$ fm, the standard rms deviation falls to $\sigma = 2.21 \times 10^{-2}$ fm. For Eq. (3), the modified formula is rewritten as,

$$R_{\text{ch}} = 0.305 + aA^{1/3} + bI + cA^{1/3}I^2 + d(N - N^*)A^{-1/2} + g(-1)^{o.e}A^{-1/2}, \quad (10)$$

$a = 0.9615$ fm, $b = -3.4264$ fm, $c = 0.9476$ fm, $d = 0.0211$ fm and $g = 0.0097$ fm, the standard rms deviation is $\sigma = 1.96 \times 10^{-2}$ fm. These lower deviations encourage us to apply the analytical formulas in describing the charge radii of superheavy nuclei.

In general, normal OES effects disclose that the charge radii of odd- N isotopes are smaller than those of their even- N neighbours. The corresponding abnormal OES effects of nuclear charge radii show a negative sign, which are also observed naturally [16]. This inverse OES in charge radii, which may be associated with the presence of octupole collectivity, is also observed apparently in astatine isotopes (See Ref. [83] and references therein). Mentioned in Ref. [84], the inverted OES is interpreted as an effect of polarization. The unpaired neutron polarizes the soft even-even core towards pronounced octupole deformation [85]. Similar arguments were used to interpret the anomalous OES in the europium isotopes with $N = 89-92$ [86]. As argued in [71], pair mean field as well as the gap potential are both responsible for the occurrence of OES in nuclear size. Since it is still a longstanding and open topic in nuclear physics. With this prescription, the introduced term is mandatory to explicate this normal OES effect in our fitting procedure. However, the shape deformation effect is excluded in recent calibration procedure.

B. Charge radii for Po, Rn and Ra isotopes

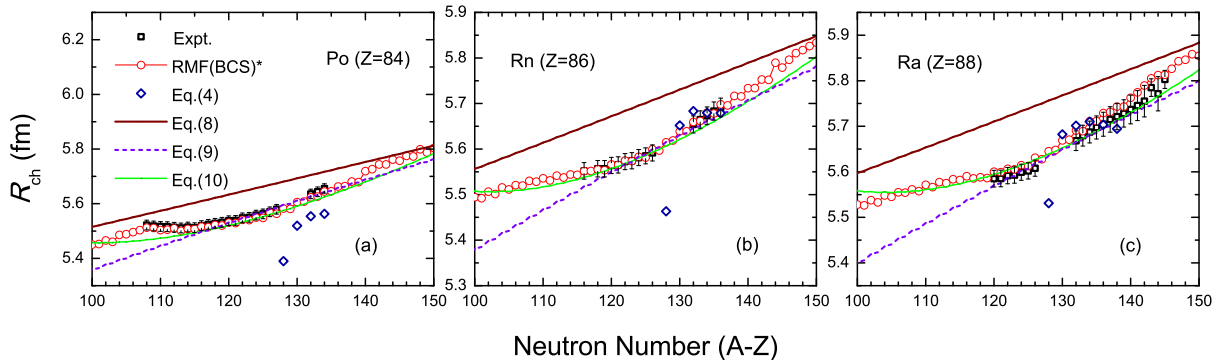


FIG. 2. Charge radii of polonium (a), radon (b) and radium (c) isotopes obtained by RMF(BCS)* approach, Eq. (4) deriving from α -decay properties and new parametrization formulas Eq. (8), Eq. (9) and Eq. (10). The experimental data are taken from Refs. [16, 17].

To facilitate the quantitative comparison of the experimental results with those from various theoretical calculations, the charge radii of polonium, radon and radium isotopes are shown in Fig. 2. One can see that the rms charge radii with RMF(BCS)* approach compare well against the experimental data. The results deduced from α -decay properties are also

in good agreement with the database except the results around $N = 126$ shell closures for Rn and Ra isotopes. For Po isotopes, the calculated results are slightly underestimated by Eq. (4), the rapid reduction occurs at $N = 128$. As mentioned in Ref. [43], shell effects bring in a reduction in the cluster formation probability, but the constant α -preformation factor cannot describe such a reduction. That is why the rms charge radii seem to be underestimated by Eq. (4) around $N = 126$ shell closure.

The calculated results are overestimated systematically by analytical formula Eq. (8) but underestimated by Eq. (9) in neutron-deficient regions. Results obtained by Eq. (10) can also reproduce the experimental data well, especially the smooth variations toward closed-shell and then the increasing trend occurs across the strong $N = 126$ shell closure. It is noted that analytical formula Eq. (10) and RMF(BCS)* approach offer the comparable results. The discrepancy in the plots with Eq. (9) becomes larger with respect to Eq. (10). The reasons are those the isospin freedom is ignored in the fitting protocol procedure and the shell closure cannot be captured well. In neutron-deficient regions, the deviation occurs between Eq. (9) and Eq. (10) due to the absence of high-order isospin freedom.

Actually, the fundamental properties of heavy or superheavy nuclei are more complex, that is not totally uncovered by our calibration procedure. The existence of such a simple curve provides guidance for characterising the nuclear size of unknown regions. This is aimed at drawing some general conclusions in these superheavy nuclei as well as their variational trends with the increase of neutron number.

C. Charge radii for even $Z = 98$ -120 isotopes

As discussed above, Eq. (8) and Eq. (9) suffer from larger uncertainties. Thus Eq. (10) is used to make further calculation in next discussions. Furthermore, the nuclear size along $Z = 98$ -120 isotopic chains are calculated by using the formula derived from α -decay properties and RMF(BCS)* approach. In Fig. 3, charge radii of even $Z = 98$ -120 isotopes are predicted by RMF(BCS)* method and analytical formulas Eq. (4) and Eq. (10). The charge radii show an increasing trend with the increase of neutron number for all isotopic chains.

The results obtained by Eq. (10) are also in good agreement with the predictions of the RMF(BCS)* approach for Cf, Fm and No isotopes. As discussed before, charge radii vary smoothly toward neutron closed-shells. and a larger increase occurs through the filling of

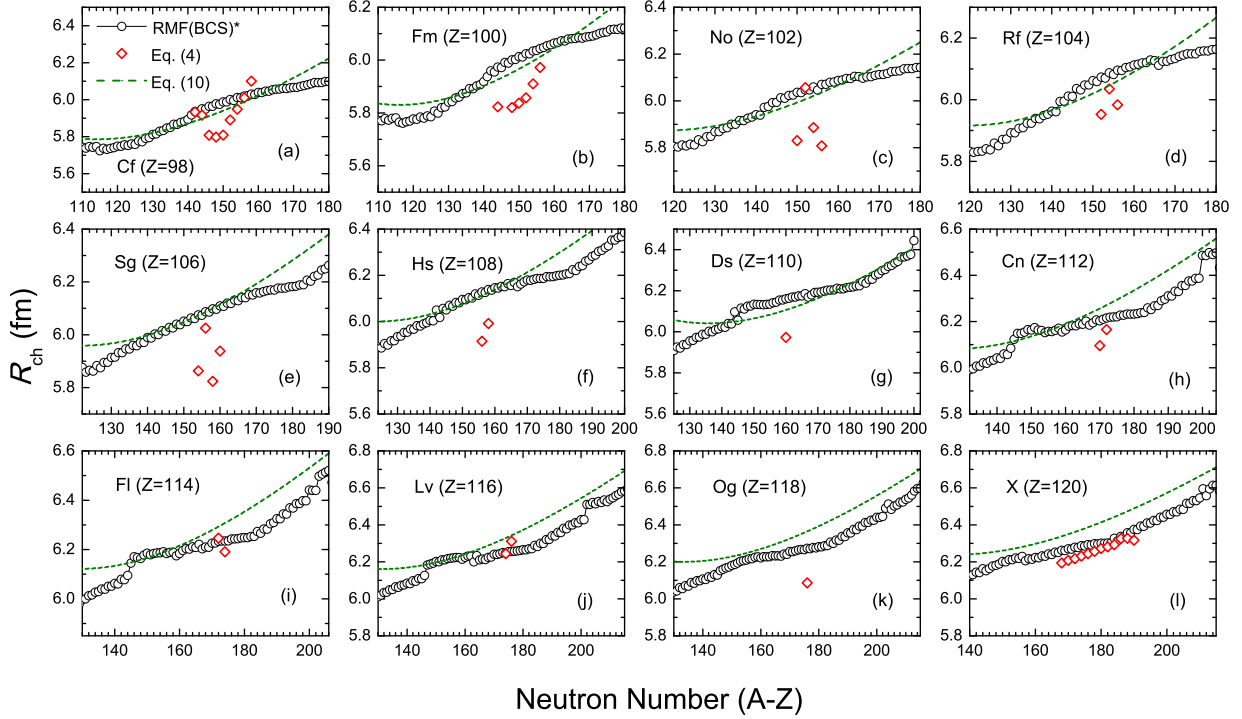


FIG. 3. The charge radii of even $Z = 98-120$ isotopes are drawn with RMF(BCS)* method and analytical formulas Eq. (4) and Eq. (10). The α -decay energy are taken from the latest evaluated atomic mass table AME2020 [87]. The experimental α -decay half-lives are taken from the latest evaluated nuclear properties table NUBASE2020 [88]. The α -decay half-lives and energy for $Z = 120$ isotopes are taken from Ref. [89].

the new open shells [19, 23, 24]. As shown in Refs. [6, 90, 91], $N = 184$ is suggested to be the magic number. In fitting protocol procedure, the shell closure effect at $N = 184$ is excluded due to the absence of database. That is why these increasing behaviors still exist beyond $N = 170$ for all this isotopes. In neutron-deficient regions, the deviation also exists between RMF(BCS)* approach and Eq. (10). Although the OES term is introduced in analytical formulas, the amplitudes of OES is decreased dramatically with the increase of mass number. Therefore, no apparently oscillatory behaviors are drawn in this quantitative level.

As a complex many-body quantum system, the remarkably abrupt changes in charge radii are observed naturally across neutron shell closures. RMF(BCS)* model can reproduce the shell effect in nuclear size fairly well for Ca, K, Cu and In isotopes [44, 65, 66], etc, especially the inverted parabolic-like behaviors between two closed-shells. This is an indication of the

shell effect along isotopic chain. In superheavy regions, as shown before $N = 184$ is suggested to be the magic number [6, 90, 91]. In Fig. 3, results obtained by RMF(BCS)* approach show a rapidly increasing phenomenon across the main neutron shell of $N = 126$ along $Z = 98$ -110 isotopic chains, the same scenario can be encountered around $N = 184$ regions along $Z = 112$ -120 isotopic chains. Between these two $N = 126$ and 184 filled-shells, the inverted parabolic-like behaviors of charge radii can be expected to be seen but with lower amplitudes.

TABLE I. The rms charge radii of $Z = 120$ isotopes obtained by RMF(BCS)*, Eq. (4) and Eq. (10) approaches (in units of fm).

| Nuclei | RMF(BCS)* | Eq. (4) | Eq. (10) |
|----------------|-----------|---------|----------|
| $^{288}_{120}$ | 6.2627 | 6.1941 | 6.3388 |
| $^{290}_{120}$ | 6.2705 | 6.2078 | 6.3503 |
| $^{292}_{120}$ | 6.2793 | 6.2172 | 6.3622 |
| $^{294}_{120}$ | 6.2875 | 6.2311 | 6.3746 |
| $^{296}_{120}$ | 6.2931 | 6.2434 | 6.3875 |
| $^{298}_{120}$ | 6.2981 | 6.2567 | 6.4009 |
| $^{300}_{120}$ | 6.3013 | 6.2726 | 6.4146 |
| $^{302}_{120}$ | 6.3023 | 6.2811 | 6.4288 |
| $^{304}_{120}$ | 6.3274 | 6.2926 | 6.4434 |
| $^{306}_{120}$ | 6.3380 | 6.3254 | 6.4584 |
| $^{308}_{120}$ | 6.3573 | 6.3269 | 6.4737 |
| $^{310}_{120}$ | 6.3757 | 6.3170 | 6.4895 |

Other interesting phenomena that nuclear charge radii appear to increase with surprisingly leaping slopes are observed remarkably around $N = 146$ and 200. As argued in Ref. [28], the abrupt changes of nuclear charge radii corresponds to the onset of deformation. Besides the abrupt changes at neutron shell closure, the changes in nuclear deformation are enough to cause the observed kink phenomena [71]. In this work, the nuclear shape are abruptly increasing from spherical to deformed around $N = 146$ and 200 regions. The corresponding quadrupole deformation parameters are $\beta_{20} \approx 0.30$, and these are consistent

with Ref. [92]. Hence the most rapid spherical-deformed phase transition may occur around $N = 146$ and 200 in superheavy regions. This means deformation effect plays a crucial role in defining the properties such as nuclear sizes and isotope shifts. However, this effect has not been included in calibration procedure. RMF(BCS)* approach with its attendant greater reliability can reproduce deformation and the inherent shell effects.

The fitting results derived from α -decay properties have a larger deviation with respect to calculations in RMF(BCS)* approach. For $^{286,288}\text{Fl}$, $^{290,292}\text{Lv}$ and $^{168-190}\text{120}$ isotopes, there is an almost unanimity in the values calculated by these three methods. In Table I, charge radii of $Z = 120$ isotopes are shown with RMF(BCS)*, Eq. (4) and Eq. (10) approaches. As mentioned above, Eq. (10) fails to follow the evolution of arch shape with the increasing of neutron number. In our protocol procedure, the shell effect is excluded at $N = 184$ due to the absence of nuclear database. In addition the shape deformation is also neglected.

IV. SUMMARY

In this work, the analytical formulas with new parametrization sets are fitted by introducing the odd-even staggering (OES) and shell closure effect. The fitted formula within theoretical uncertainty below 0.02 fm can reproduce the experimental data, especially the shell effect at $N = 126$. Furthermore, the high-order isospin symmetry freedom may be necessary in calibration procedure. Charge radii of nuclei with even $Z = 98 - 120$ isotopes are calculated systematically by various approaches including the analytical formula as a function of mass number, deduced relation associated to α -decay properties and RMF(BCS)* approach. The abrupt changes of nuclear charge radii at $N = 184$ shells are shown apparently by RMF(BCS)* approach. Besides, the inverted parabolic-like behaviors between $N = 126$ and 184 shell closures are also shown but with slight amplitudes.

Actually, nuclear charge radii are influenced by various mechanisms, such the high order moment [93, 94], spherical-deformed phase transition [95], pairing component [72], $N_p N_n$ scheme that describes the proton-neutron interaction [96], etc. As shown in Ref. [97] that the density dependent pairing may also induce sizeable staggering and kinks in the evolution of the nuclear charge radii. As shown in Fig. 1, the abrupt changes of nuclear charge radii are indicated in $A = 100$, 150 and 190 regions [27]. Results obtained by RMF(BCS)* approach show a remarkable similarity that deformation phase transition regions are also

shown around $N = 146$ and 200 regions. These curves for respective transition regions can be used to guide further test.

V. ACKNOWLEDGEMENTS

This work is supported in part by the Reform and Development Project of Beijing Academy of Science and Technology under Grant No. 13001-2110, the National Natural Science Foundation of China (NSFC) under Grants No. 12135004, No. 11635003, No. 11025524, No. 11161130520, the National Basic Research Program of China under Grant No. 2010CB832903.

-
- [1] M. S. Safronova, D. Budker, D. DeMille, D. F. J. Kimball, A. Derevianko, and C. W. Clark, *Rev. Mod. Phys.* **90**, 025008 (2018).
 - [2] M. Arnould and S. Goriely, *Prog. Part. Nucl. Phys.* **112**, 103766 (2020).
 - [3] B. A. Brown, *Phys. Rev. Lett.* **119**, 122502 (2017).
 - [4] J. Yang and J. Piekarewicz, *Phys. Rev. C* **97**, 014314 (2018).
 - [5] Y. T. Oganessian, F. S. Abdullin, C. Alexander, J. Binder, R. A. Boll, S. N. Dmitriev, J. Ezold, K. Felker, J. M. Gostic, R. K. Grzywacz, J. H. Hamilton, R. A. Henderson, M. G. Itkis, K. Miernik, D. Miller, K. J. Moody, A. N. Polyakov, A. V. Ramayya, J. B. Roberto, M. A. Ryabinin, K. P. Rykaczewski, R. N. Sagaidak, D. A. Shaughnessy, I. V. Shirokovsky, M. V. Shumeiko, M. A. Stoyer, N. J. Stoyer, V. G. Subbotin, A. M. Sukhov, Y. S. Tsyganov, V. K. Utyonkov, A. A. Voinov, and G. K. Vostokin, *Phys. Rev. Lett.* **109**, 162501 (2012).
 - [6] Y. T. Oganessian and V. K. Utyonkov, *Rep. Prog. Phys.* **78**, 036301 (2015).
 - [7] R. Hofstadter, H. R. Fechter, and J. A. McIntyre, *Phys. Rev.* **92**, 978 (1953).
 - [8] R. G. Arnold, C. E. Carlson, and F. Gross, *Phys. Rev. C* **21**, 1426 (1980).
 - [9] R. Engfer, H. Schnewly, J. L. Vuilleumier, H. K. Walter, and A. Zehnder, *At. Data Nucl. Data Tables* **14**, 509 (1974), [Erratum: *At. Data Nucl. Data Tables* **16**, 580–580 (1975)].
 - [10] G. Fricke, C. Bernhardt, K. Heilig, L. Schaller, L. Schellenberg, E. Shera, and C. Dejager, *At. Data Nucl. Data Tables* **60**, 177 (1995).

- [11] M. Bazzi, G. Beer, L. Bombelli, A. Bragadireanu, M. Cargnelli, G. Corradi, C. Curceanu (Petrascu), A. d’Uffizi, C. Fiorini, T. Frizzi, F. Ghio, B. Girolami, C. Guaraldo, R. Hayano, M. Iliescu, T. Ishiwatari, M. Iwasaki, P. Kienle, P. Levi Sandri, A. Longoni, J. Marton, S. Okada, D. Pietreanu, T. Ponta, A. Rizzo, A. Romero Vidal, A. Scordo, H. Shi, D. Sirghi, F. Sirghi, H. Tatsuno, A. Tudorache, V. Tudorache, O. Vazquez Doce, E. Widmann, B. Wünschek, and J. Zmeskal, *Phys. Lett.* **B697**, 199 (2011).
- [12] T. E. Cocolios, H. H. Al Suradi, J. Billowes, I. Budinčević, R. P. de Groote, S. De Schepper, V. N. Fedosseev, K. T. Flanagan, S. Franchoo, R. F. Garcia Ruiz, H. Heylen, F. Le Blanc, K. M. Lynch, B. A. Marsh, P. J. R. Mason, G. Neyens, J. Papuga, T. J. Procter, M. M. Rajabali, R. E. Rossel, S. Rothe, G. S. Simpson, A. J. Smith, I. Strashnov, H. H. Stroke, D. Verney, P. M. Walker, K. D. A. Wendt, and R. T. Wood, *Nucl. Instrum. Meth. B* **317**, 565 (2013).
- [13] A. R. Vernon, C. M. Ricketts, J. Billowes, T. E. Cocolios, B. S. Cooper, K. T. Flanagan, R. F. Garcia Ruiz, F. P. Gustafsson, G. Neyens, H. A. Perrett, B. K. Sahoo, Q. Wang, F. J. Waso, and X. F. Yang, *Sci. Rep.* **10**, 12306 (2020).
- [14] I. Angeli, *At. Data Nucl. Data Tables* **87**, 185 (2004).
- [15] S. Q. Zhang, J. Meng, S. G. Zhou, and J. Y. Zeng, *Eur. Phys. J. A* **13**, 285 (2002).
- [16] I. Angeli and K. Marinova, *At. Data Nucl. Data Tables* **99**, 69 (2013).
- [17] T. Li, Y. Luo, and N. Wang, *At. Data Nucl. Data Tables* **140**, 101440 (2021).
- [18] A. J. Miller, K. Minamisono, A. Klose, D. Garand, C. Kujawa, J. D. Lantis, Y. Liu, B. Maaß, P. F. Mantica, W. Nazarewicz, W. Nörtershäuser, S. V. Pineda, P.-G. Reinhard, D. M. Rossi, F. Sommer, C. Sumithrarachchi, A. Teigelhöfer, and J. Watkins, *Nature Phys.* **15**, 432 (2019).
- [19] R. F. Garcia Ruiz, M. L. Bissell, K. Blaum, A. Ekström, N. Frömmgen, G. Hagen, M. Hammen, K. Hebel, J. D. Holt, G. R. Jansen, M. Kowalska, K. Kreim, W. Nazarewicz, R. Neugart, G. Neyens, W. Nörtershäuser, T. Papenbrock, J. Papuga, A. Schwenk, J. Simonis, K. A. Wendt, and D. T. Yordanov, *Nature Phys.* **12**, 594 (2016).
- [20] T. Day Goodacre, A. V. Afanasjev, A. E. Barzakh, B. A. Marsh, S. Sels, P. Ring, H. Nakada, A. N. Andreyev, P. Van Duppen, N. A. Althubiti, B. Andel, D. Atanasov, J. Billowes, K. Blaum, T. E. Cocolios, J. G. Cubiss, G. J. Farooq-Smith, D. V. Fedorov, V. N. Fedosseev, K. T. Flanagan, L. P. Gaffney, L. Ghys, M. Huysse, S. Kreim, D. Lunney, K. M. Lynch, V. Manea, Y. Martinez Palenzuela, P. L. Molkanov, M. Rosenbusch, R. E. Rossel, S. Rothe,

- L. Schweikhard, M. D. Seliverstov, P. Spagnoletti, C. Van Beveren, M. Veinhard, E. Verstraelen, A. Welker, K. Wendt, F. Wienholtz, R. N. Wolf, A. Zadvornaya, and K. Zuber, *Phys. Rev. Lett.* **126**, 032502 (2021).
- [21] M. Anselment, W. Faubel, S. Göring, A. Hanser, G. Meisel, H. Rebel, and G. Schatz, *Nucl. Phys. A* **451**, 471 (1986).
- [22] Á. Koszorús, X. F. Yang, W. G. Jiang, S. J. Novario, S. W. Bai, J. Billowes, C. L. Binnie, M. L. Bissell, T. E. Cocolios, B. S. Cooper, R. P. de Grootz, A. Ekström, K. T. Flanagan, C. Forssén, S. Franchoo, R. F. G. Ruiz, F. P. Gustafsson, G. Hagen, G. R. Jansen, A. Kanellakopoulos, M. Kortelainen, W. Nazarewicz, G. Neyens, T. Papenbrock, P.-G. Reinhard, B. K. Sahoo, C. M. Ricketts, A. R. Vernon, and S. G. Wilkins, *Nature Phys.* **17**, 439 (2021), [Erratum: *Nature Phys.* **17**, 539 (2021)], [arXiv:2012.01864 \[nucl-ex\]](https://arxiv.org/abs/2012.01864).
- [23] C. Gorges, L. V. Rodríguez, D. L. Balabanski, M. L. Bissell, K. Blaum, B. Cheal, R. F. Garcia Ruiz, G. Georgiev, W. Gins, H. Heylen, A. Kanellakopoulos, S. Kaufmann, M. Kowalska, V. Lagaki, S. Lechner, B. Maaß, S. Malbrunot-Ettenauer, W. Nazarewicz, R. Neugart, G. Neyens, W. Nörtershäuser, P.-G. Reinhard, S. Sailer, R. Sánchez, S. Schmidt, L. Wehner, C. Wraith, L. Xie, Z. Y. Xu, X. F. Yang, and D. T. Yordanov, *Phys. Rev. Lett.* **122**, 192502 (2019).
- [24] R. F. Garcia Ruiz and A. R. Vernon, *Eur. Phys. J. A* **56**, 136 (2020).
- [25] M. Bhuyan, B. Maheshwari, H. A. Kassim, N. Yusof, S. K. Patra, B. V. Carlson, and P. D. Stevenson, *J. Phys. G: Nucl. Part. Phys.* **48**, 075105 (2021).
- [26] G. A. Lalazissis, M. M. Sharma, and P. Ring, *Nucl. Phys. A* **597**, 35 (1996).
- [27] R. F. Casten, *Phys. Rev. Lett.* **54**, 1991 (1985).
- [28] T. Togashi, Y. Tsunoda, T. Otsuka, and N. Shimizu, *Phys. Rev. Lett.* **117**, 172502 (2016).
- [29] M. Bender, P.-H. Heenen, and P.-G. Reinhard, *Rev. Mod. Phys.* **75**, 121 (2003).
- [30] L.-S. Geng, H. Toki, S. Sugimoto, and J. Meng, *Prog. Theor. Phys.* **110**, 921 (2003).
- [31] P. W. Zhao, Z. P. Li, J. M. Yao, and J. Meng, *Phys. Rev. C* **82**, 054319 (2010).
- [32] X. Xia, Y. Lim, P. Zhao, H. Liang, X. Qu, Y. Chen, H. Liu, L. Zhang, S. Zhang, Y. Kim, and J. Meng, *At. Data Nucl. Data Tables* **121-122**, 1 (2018).
- [33] K. Zhang, M.-K. Cheoun, Y.-B. Choi, P. S. Chong, J. Dong, L. Geng, E. Ha, X. He, C. Heo, M. C. Ho, E. J. In, S. Kim, Y. Kim, C.-H. Lee, J. Lee, Z. Li, T. Luo, J. Meng, M.-H. Mun, Z. Niu, C. Pan, P. Papakonstantinou, X. Shang, C. Shen, G. Shen, W. Sun, X.-X. Sun, C. K.

- Tam, Thavayongnong, C. Wang, S. H. Wong, X. Xia, Y. Yan, R. W.-Y. Yeung, T. C. Yiu, S. Zhang, W. Zhang, and S.-G. Zhou (DRHBc Mass Table Collaboration), *Phys. Rev. C* **102**, 024314 (2020).
- [34] K. Zhang, X. He, J. Meng, C. Pan, C. Shen, C. Wang, and S. Zhang, *Phys. Rev. C* **104**, 021301 (2021).
- [35] S. Goriely, N. Chamel, and J. M. Pearson, *Phys. Rev. C* **82**, 035804 (2010).
- [36] S. Goriely, S. Hilaire, M. Girod, and S. Péru, *Phys. Rev. Lett.* **102**, 242501 (2009).
- [37] S. Binder, J. Langhammer, A. Calci, and R. Roth, *Phys. Lett.* **B736**, 119 (2014).
- [38] A. Ekström, G. R. Jansen, K. A. Wendt, G. Hagen, T. Papenbrock, B. D. Carlsson, C. Forssén, M. Hjorth-Jensen, P. Navrátil, and W. Nazarewicz, *Phys. Rev. C* **91**, 051301 (2015).
- [39] J. Simonis, S. R. Stroberg, K. Hebeler, J. D. Holt, and A. Schwenk, *Phys. Rev. C* **96**, 014303 (2017).
- [40] R. Utama, W.-C. Chen, and J. Piekarewicz, *J. Phys. G: Nucl. Part. Phys.* **43**, 114002 (2016).
- [41] X.-X. Dong, R. An, J.-X. Lu, and L.-S. Geng, (2021), [arXiv:2109.09626 \[nucl-th\]](https://arxiv.org/abs/2109.09626).
- [42] F.-S. Zhang, C. Li, L. Zhu, and P. W. Wen, *Front. Phys.* **13**, 132113 (2018).
- [43] D. Ni, Z. Ren, T. Dong, and Y. Qian, *Phys. Rev. C* **87**, 024310 (2013).
- [44] R. An, L.-S. Geng, and S.-S. Zhang, *Phys. Rev. C* **102**, 024307 (2020).
- [45] B. Nerlo-Pomorska and K. Pomorski, *Z. Phys. A* **348**, 169 (1994).
- [46] W. D. Myers and W. J. Świątecki, *Phys. Rev. C* **62**, 044610 (2000).
- [47] G. Royer, *Nucl. Phys. A* **807**, 105 (2008).
- [48] Z. Sheng, G. Fan, J. Qian, and J. Hu, *Eur. Phys. J. A* **51**, 40 (2015).
- [49] J. Piekarewicz, M. Centelles, X. Roca-Maza, and X. Vinas, *Eur. Phys. J. A* **46**, 379 (2010).
- [50] Y. Ma, C. Su, J. Liu, Z. Ren, C. Xu, and Y. Gao, *Phys. Rev. C* **101**, 014304 (2020).
- [51] Y. Qian, Z. Ren, and D. Ni, *Phys. Rev. C* **87**, 054323 (2013).
- [52] D. Vretenar, A. V. Afanasjev, G. A. Lalazissis, and P. Ring, *Phys. Rept.* **409**, 101 (2005).
- [53] Q. Zhao, J. M. Dong, J. L. Song, and W. H. Long, *Phys. Rev. C* **90**, 054326 (2014).
- [54] H. Liang, J. Meng, and S.-G. Zhou, *Phys. Rept.* **570**, 1 (2015).
- [55] S. S. Zhang, W. Zhang, S. G. Zhou, and J. Meng, *Eur. Phys. J. A* **32**, 43 (2007).
- [56] P. W. Zhao, J. Peng, H. Z. Liang, P. Ring, and J. Meng, *Phys. Rev. C* **85**, 054310 (2012).
- [57] S.-G. Zhou, J. Meng, and P. Ring, *Phys. Rev. C* **68**, 034323 (2003).
- [58] S.-G. Zhou, J. Meng, P. Ring, and E.-G. Zhao, *Phys. Rev. C* **82**, 011301 (2010).

- [59] J. Meng, H. Toki, S. G. Zhou, S. Q. Zhang, W. H. Long, and L. S. Geng, *Prog. Part. Nucl. Phys.* **57**, 470 (2006).
- [60] L.-G. Cao and Z.-Y. Ma, *Eur. Phys. J. A* **22**, 189 (2004).
- [61] S.-S. Zhang, X.-D. Xu, and J.-P. Peng, *Eur. Phys. J. A* **48**, 40 (2012).
- [62] R. An, G.-F. Shen, S.-S. Zhang, and L.-S. Geng, *Chin. Phys. C* **44**, 074101 (2020).
- [63] Y. K. Gambhir, P. Ring, and A. Thimet, *Ann. Phys.* **198**, 132 (1990).
- [64] P. Ring, Y. K. Gambhir, and G. A. Lalazissis, *Comput. Phys. Commun.* **105**, 77 (1997).
- [65] R. An, S.-S. Zhang, L.-S. Geng, and F.-S. Zhang, (2021), [arXiv:2106.02279 \[nucl-th\]](#).
- [66] R. An, X. Jiang, L.-G. Cao, and F.-S. Zhang, (2021), [arXiv:2107.05057 \[nucl-th\]](#).
- [67] G. A. Lalazissis, J. König, and P. Ring, *Phys. Rev. C* **55**, 540 (1997).
- [68] G. A. Miller, A. Beck, S. May-Tal Beck, L. B. Weinstein, E. Piasezky, and O. Hen, *Phys. Lett.* **B793**, 360 (2019).
- [69] R. An, X. Jiang, L.-G. Cao, and F.-S. Zhang, (2021), [arXiv:2108.00278 \[nucl-th\]](#).
- [70] U. C. Perera, A. V. Afanasjev, and P. Ring, (2021), [arXiv:2108.02245 \[nucl-th\]](#).
- [71] S. Sakakihara and Y. Tanaka, *Nucl. Phys. A* **691**, 649 (2001).
- [72] P.-G. Reinhard and W. Nazarewicz, *Phys. Rev. C* **95**, 064328 (2017).
- [73] I. N. Borzov and S. V. Tolokonnikov, *Phys. Atom. Nucl.* **83**, 828 (2020).
- [74] P. Brix and H. Kopfermann, *Rev. Mod. Phys.* **30**, 517 (1958).
- [75] B. A. Marsh, T. Day Goodacre, S. Sels, Y. Tsunoda, B. Andel, A. N. Andreyev, N. A. Althubiti, D. Atanasov, A. E. Barzakh, J. Billowes, K. Blaum, T. E. Cocolios, J. G. Cubiss, J. Dobaczewski, G. J. Farooq-Smith, D. V. Fedorov, V. N. Fedosseev, K. T. Flanagan, L. P. Gaffney, L. Ghys, M. Huyse, S. Kreim, D. Lunney, K. M. Lynch, V. Manea, Y. Martinez Palenzuela, P. L. Molkanov, T. Otsuka, A. Pastore, M. Rosenbusch, R. E. Rossel, S. Rothe, L. Schweikhard, M. D. Seliverstov, P. Spagnoletti, C. Van Beveren, P. Van Duppen, M. Veinhard, E. Verstraelen, A. Welker, K. Wendt, F. Wienholtz, R. N. Wolf, A. Zadvornaya, and K. Zuber, *Nature Phys.* **14**, 1163 (2018).
- [76] S. Péru, S. Hilaire, S. Goriely, and M. Martini, *Phys. Rev. C* **104**, 024328 (2021).
- [77] A. Barzakh, A. N. Andreyev, C. Raison, J. G. Cubiss, P. Van Duppen, S. Péru, S. Hilaire, S. Goriely, B. Andel, S. Antalic, M. Al Monthery, J. C. Berengut, J. Bieroń, M. L. Bissell, A. Borschevsky, K. Chrysalidis, T. E. Cocolios, T. Day Goodacre, J.-P. Dognon, M. Elantkowska, E. Eliav, G. J. Farooq-Smith, D. V. Fedorov, V. N. Fedosseev, L. P. Gaffney, R. F.

- Garcia Ruiz, M. Godefroid, C. Granados, R. D. Harding, R. Heinke, M. Huyse, J. Karls, P. Larmonier, J. G. Li, K. M. Lynch, D. E. Maison, B. A. Marsh, P. Molkanov, P. Mosat, A. V. Oleynichenko, V. Panteleev, P. Pyykkö, M. L. Reitsma, K. Rezyunkina, R. E. Rossel, S. Rothe, J. Ruczkowski, S. Schiffmann, C. Seiffert, M. D. Seliverstov, S. Sels, L. V. Skripnikov, M. Stryczyk, D. Studer, M. Verlinde, S. Wilman, and A. V. Zaitsevskii, *Phys. Rev. Lett.* **127**, 192501 (2021).
- [78] A. L. Goodman, *Nucl. Phys. A* **287**, 1 (1977).
- [79] P. Ring and P. Schuck, *The Nuclear Many-Body Problem* (Springer-Verlag, New York, 1980).
- [80] R. F. Casten, D. S. Brenner, and P. E. Haustein, *Phys. Rev. Lett.* **58**, 658 (1987).
- [81] I. Angeli, *J. Phys. G: Nucl. Part. Phys.* **17**, 439 (1991).
- [82] N. Wang and T. Li, *Phys. Rev. C* **88**, 011301 (2013).
- [83] A. E. Barzakh, J. G. Cubiss, A. N. Andreyev, M. D. Seliverstov, B. Andel, S. Antalic, P. Ascher, D. Atanasov, D. Beck, J. Bieroń, K. Blaum, C. Borgmann, M. Breitenfeldt, L. Capponi, T. E. Cocolios, T. Day Goodacre, X. Derkx, H. De Witte, J. Elseviers, D. V. Fedorov, V. N. Fedoseev, S. Fritzsche, L. P. Gaffney, S. George, L. Ghys, F. P. Heßberger, M. Huyse, N. Imai, Z. Kalaninová, D. Kisler, U. Köster, M. Kowalska, S. Kreim, J. F. W. Lane, V. Liberati, D. Lunney, K. M. Lynch, V. Manea, B. A. Marsh, S. Mitsuoka, P. L. Molkanov, Y. Nagame, D. Neidherr, K. Nishio, S. Ota, D. Pauwels, L. Popescu, D. Radulov, E. Rapisarda, J. P. Revill, M. Rosenbusch, R. E. Rossel, S. Rothe, K. Sandhu, L. Schweikhard, S. Sels, V. L. Truesdale, C. Van Beveren, P. Van den Bergh, P. Van Duppen, Y. Wakabayashi, K. D. A. Wendt, F. Wienholtz, B. W. Whitmore, G. L. Wilson, R. N. Wolf, and K. Zuber, *Phys. Rev. C* **99**, 054317 (2019).
- [84] P. Lievens, E. Arnold, W. Borchers, U. Georg, M. Keim, A. Klein, R. Neugart, L. Vermeeren, and R. E. Silverans, *Europhys. Lett.* **33**, 11 (1996).
- [85] S. Ahmad, W. Klempt, R. Neugart, E. Otten, P.-G. Reinhard, G. Ulm, and K. Wendt, *Nucl. Phys. A* **483**, 244 (1988).
- [86] G. D. Alkhazov, A. E. Barzakh, V. A. Bolshakov, V. P. Denisov, V. S. Ivanov, Y. Y. Sergeev, I. Y. Chubukov, V. I. Tikhonov, V. S. Letokhov, V. I. Mishin, S. K. Sekatsky, and V. N. Fedoseyev, *Z. Phys. A* **337**, 257 (1990).
- [87] W. Huang, M. Wang, F. Kondev, G. Audi, and S. Naimi, *Chin. Phys. C* **45**, 030002 (2021).

- [88] F. G. Kondev, M. Wang, W. J. Huang, S. Naimi, and G. Audi, *Chin. Phys. C* **45**, 030001 (2021).
- [89] J.-G. Deng, H.-F. Zhang, and G. Royer, *Phys. Rev. C* **101**, 034307 (2020).
- [90] M. W. Kirson, *Nucl. Phys. A* **798**, 29 (2008).
- [91] W. Zhang, J. Meng, S. Zhang, L. Geng, and H. Toki, *Nucl. Phys. A* **753**, 106 (2005).
- [92] P. Möller, A. J. Sierk, T. Ichikawa, and H. Sagawa, *At. Data Nucl. Data Tables* **109-110**, 1 (2016).
- [93] P.-G. Reinhard, W. Nazarewicz, and R. F. Garcia Ruiz, *Phys. Rev. C* **101**, 021301 (2020).
- [94] T. Naito, G. Colò, H. Liang, and X. Roca-Maza, *Phys. Rev. C* **104**, 024316 (2021).
- [95] P.-G. Reinhard and W. Nazarewicz, *Phys. Rev. C* **103**, 054310 (2021).
- [96] R. F. Casten, *Phys. Rev. C* **33**, 1819 (1986).
- [97] S. Fayans, S. Tolokonnikov, E. Trykov, and D. Zawischa, *Nucl. Phys. A* **676**, 49 (2000).